Investigation of the screen printed contacts of silicon solar cells using Transmission Line Model

L.A. Dobrzański [a,*], M. Musztyfaga [a], A. Drygała [a], P. Panek [b]

[a] Division of Materials Processing Technology, Management and Computer Techniques in Materials Science, Institute of Engineering Materials and Biomaterials, Silesian University of Technology, ul. Konarskiego 18a, 44-100 Gliwice, Poland
[b] Institute of Metallurgy and Materials Science of Polish Academy of Sciences, ul. Reymonta 25, 30-059 Kraków, Poland
* Corresponding author: E-mail address: leszek.dobrzanski@polsl.pl

Properties

ABSTRACT

Purpose: The aim of the paper is to analyze how to improve the quality of the screen printed contacts of silicon solar cells. This means forming front side grid in order to decrease contact resistance.

Design/methodology/approach: The topography of screen printed contacts were investigated using ZEISS SUPRA 25 scanning electron microscope (SEM) with an energy dispersive X-ray (EDS) spectrometer for microchemical analysis. Front collection grid was created using two types of Ag pastes. The Transmission Line Model (TLM) patterns were fabricated by screen printing method on p – type Czochralski silicon Cz-Si wafer with n+ emitter without texture and with a titanium oxide (TiO$_x$) layer as an antireflection coating (ARC). Electrical properties of contacts were investigated using TLM.

Findings: This work presents a conventional analysis of a screen printing process for contact formation in the crystalline silicon solar cells. The seed layer was created using silver pasts by the screen printed metallization. These contact structures were investigated using SEM to gain a better understanding of the obtained electrical parameters.

Research limitations/implications: The contact resistance of the screen-printed metallization depends not only on the kind of applied paste and firing conditions, but is also strongly influenced by the surface morphology of the silicon substrate.

Practical implications: Contact formation is an important production step to be optimized in the development of high efficiency solar cells.

Originality/value: The effect of co-firing different pasts (especially a past, which was prepared using silver nano-powder) on electrical properties of silicon wafers.

Keywords: Electrical Properties; Solar cells; Photovoltaics; Screen-printing; Transmission Line Model

1. Introduction

Solar cell metallization is a major efficiency limiting and cost determining step in solar cell processing. Figure 1 presents a classification of the different methods used for front and back contact formation [1-14]. Screen printing is the most widely used contact formation technique for commercial Si solar cells (Fig. 2) [15]. Most screen-printed solar cells manufactured in the industry today are using the process, which consists of a relatively small number of process steps. Figure 3 presents a structure of this type of solar cell. The screen printing consists of three steps:

- overprint collection back contacts (Al/Ag) and drying,
- overprint a front contact (Ag) and drying,
- firing both front and back contacts.

Drying is applied to obtain higher stability of the print by eliminating humidity before firing. The temperature of firing is in a range from 600 °C to 900 °C for the common thin-layers silicon wafers. These temperatures are high enough to change the silicon under the contact. The optimal print of the front side is 60 μm wide and 10-15 μm high. To avoid prints defects it is necessary to control the print during the screen printing. For instance irregular width of the print can be caused by the damaged membrane of screen or unsuitable speed or the wrong angle of a squeegee spreading paste. At present, standard silicon solar cells with screen printed contacts achieve efficiency equal to 15% for polycrystalline and 16.5% for monocrystalline cells [10, 15, 16].

2. Experimental procedure

The industrial technology of monocrystalline silicon solar cells has been developed using silicon produced by Deutsche Solar (Germany) as the base material. The basic parameters of silicon used in experiments are presented in Table 1. The fabrication sequence of monocrystalline solar cells is presented in Fig. 4. The technology used to produce solar cell was performed in the Institute of Metallurgy and Materials Science of the Polish Academy of sciences (IMMS PAS).

Table 1.
Base material parameters

The basic parameters of monocrystalline silicon	
Type	p
Doped	boron
Thickness	200 ± 30 μm
Area	5x5cm
Resistivity	1 - 3 Ωcm
Carbon concentration	$8x10^{16}$ atoms/cm^3
Oxygen concentration	$1x10^{18}$ atoms/cm^3

2.1. Chemical treatment of monocrystalline wafers

To eliminate saw damage, and remove contamination and native oxides from wafers surface chemical treatment was applied. The chemical procedure applied before the donor doping process is given in Table 2.
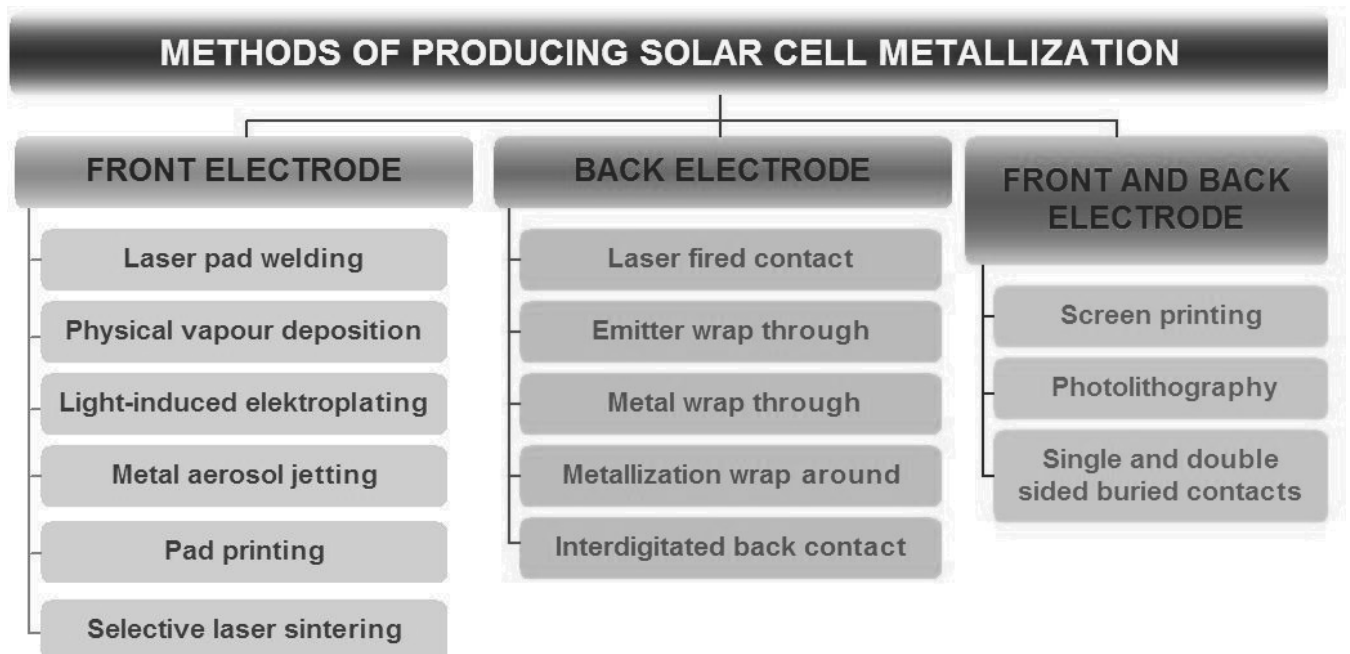
Fig. 1. Classification of the different methods used for producing solar cell contacts
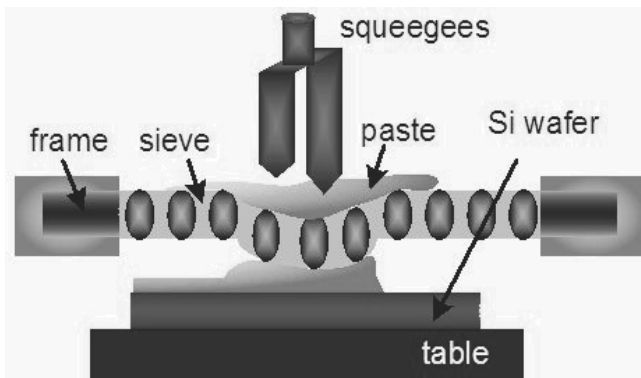
Fig. 2. The screen printing method [15]
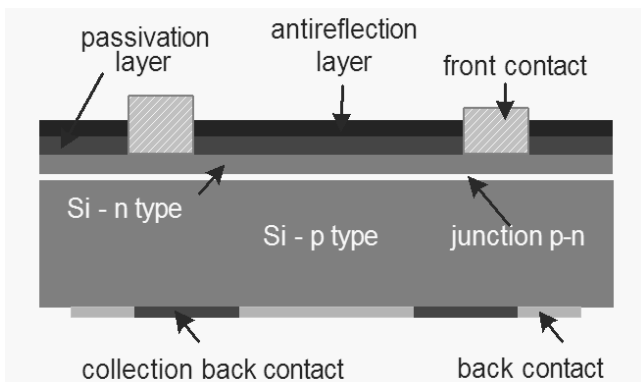
Fig. 3. Structure of a solar cell with screen-printed front and back contacts [15, 16]

Table 2.
Chemical processing of silicon wafers prior to diffusion

Chemical process	Chemical recipe	Time (min)	Temp. (°C)
Washing in acetone	CH_3COCH_3	10	56
Rinsing	DIH_2O	0,5	21
Distorted layer removing	30% KOH	3	81
Rinsing	DIH_2O	1	50
Metallic contamination removing	2%HCl	10	25
Native oxide removing	10%HF	10	25
Rinsing	DIH_2O	10	25

2.2. The p-n junction formation

One of the most important steps in the manufacturing process of silicon solar cells is emitter diffusion. The emitter was formed by diffusion in a quartz-tube type furnace at 840 °C for 40 minutes using liquid $POCl_3$ as a doping source (Fig. 5).
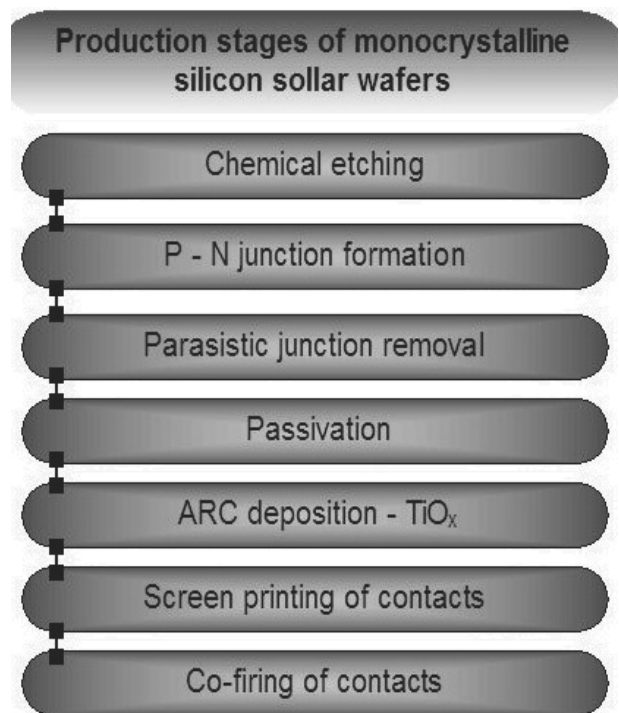
Fig. 4. Production stages of the monocrystalline solar cells at IMMS PAS

Fig. 5. PIE, SD-3/158M type diffusion furnace in IMMS PAS

2.3. Parasitic junction removal and chemical etching

The wafers were put in a pile and located in a special Teflon clamp which protects the wafer surfaces from etching. The parasitic junction was removed when a clamp was immersed in 27%HF:45%HNO$_3$:27%CH$_3$COOH solution in the volume ratio 3:5:3 for 40 seconds, followed by rising in DIH$_2$O.

After diffusion from POCl$_3$, the wafers were covered by phosphorous–silicate glass (xSiO$_2$•yP$_2$O$_5$), which was removed by immersion in a bath of 10% HF for 2 minutes.

2.4. Passivation

The surface passivation was obtained by thermal growth of a thin, transparent passivating layer of silicon dioxide (SiO$_2$) at temperature of 800 °C for 10 minutes in a controlled atmosphere of O$_2$ and N$_2$.

2.5. Antireflection coating deposition

Reducing reflection losses of the front surface of solar cell has crucial influence on its efficiency. An improvement in this area can be achieved by forming an antireflection coating (ARC). Properly chosen and deposited ARC enables to reduce the solar cell reflection below 10%. Titanium oxide (TiO$_x$) and silicon nitride (Si$_x$N$_y$) are two most often used in industry antireflection coatings. Only TiO$_x$ was deposited before contacts were screen-printed on the front side of solar cells. TiO$_x$ was deposited by spraying the tetraethylorthotitanat ((C$_2$H$_5$O)$_4$Ti) at 300 °C using purified air as a carrying gas.

2.6. Screen printed front contacts

The screen printing is very often used in photovoltaic industry to form contacts of solar cells. The first silver paste PV145 (manufactured by Du Pont) was used to form the front contact (Fig. 6). The second silver paste (nano powder + organic carrier) was used also to form the front contact. Figure 6 presents SEM micrograph of silver nano-powder. The front paths were printed using 325 mesh screens. A special test structure was prepared. The metal contacts are 20 mm wide and 10 mm long with spacing of 20 mm, 10 mm, 5 mm, 2.5 mm in between. Testing structure was prepared to evaluate the contact resistance of the metal-semiconductor junction.

2.7. Co—firing of metal front contacts

Before co-firing of metal front contacts, both the wafers with printed past and silver powder were drying in a KBC-2W dryer (manufactured by Wamed) at 130 ℃ for 15 minutes.

Infrared belt IR furnace with fitted tungsten filament lamps were used for co-firing front contact. The IR furnace is presented in Figure 7. Conveyor-belt consists of the following three temperature firing zones:

- I – 530 ˚C, lenght – 18 cm,
- II – 570 ˚C, lenght – 36 cm,
- III – 920 ˚C, length – 18 cm.

The belt speed was 200 cm/min. The technical parameters of co-firing are presented in Table 3.
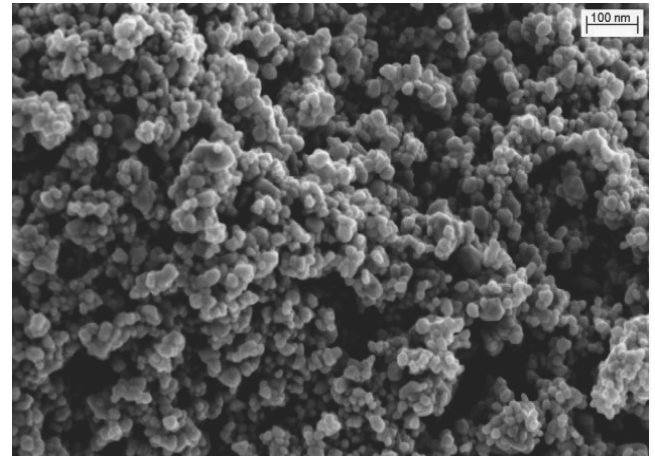
Fig. 6. SEM Micrograph of silver nano-powder

Fig. 7. LA-310 RTC type IR furnace at IMMS PAS

L.A. Dobrzański, M. Musztyfaga, A. Drygała, P. Panek

Table 3.
Parameters for the co-firing in the IR furnace

Type	Zone		
	I	II	III
	Temperature [°C]		
Monocrystalline solar cells with TiO$_x$	530	570	920

2.8. Transmission Line Model measurements

The contact resistance is characterized by two parameters [17, 18]:
- the specific contact resistance ρ_c [Ωcm^2],
- the sheet resistance R_p [Ω/Υ].

The specific contact resistance defines not only the real joint zone of contact with Si substrate, but the regions directly under and below surface of phase separation. The quality of ohmic contact to semiconductor can be studied by measuring the value of specific contact resistance. For ohmic contact, this parameter can be determined by the Transmission Line Method (TLM). In this method, the contact resistance (R) between any two separate contacts is measured (Fig. 8) and calculated with using a general formula [18]:

$$R = 2R_c + \frac{d \cdot R_p}{k} \quad [\Omega] \tag{1}$$

where: k – front contact length, $d_{1..n}$ – distance between paths of contacts, R$_c$ – contact resistance, L – width of contact
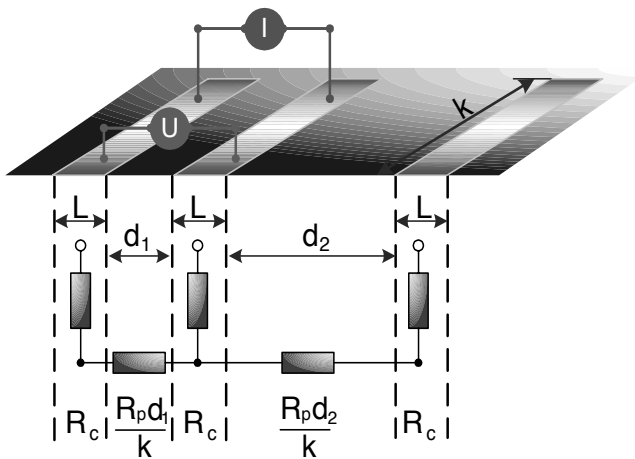
Fig. 8. Standard structure for TLM measurements, where: L-width of contact [18]

The contact resistance (R) of front contact can be determined from a chart $R = f(d)$ (Fig. 9).
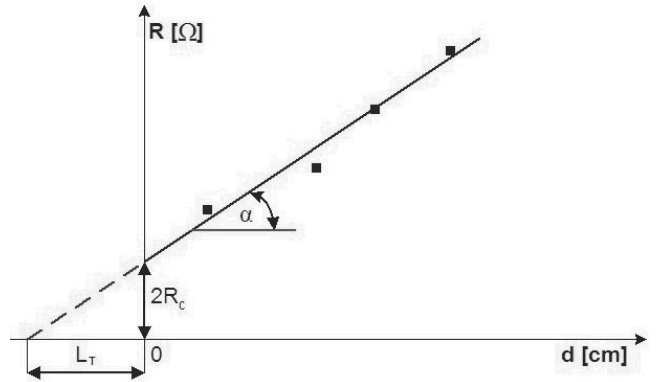
Fig. 9. Typical graphic method used to determine factors (L_T, R_c), where L_T– transfer length [17]

The resistance of front contact was calculated from equation (1), but other parameters like R_c and L_T were calculated from the linear regression. The specific contact resistance was calculated according to conditions [17]:

If $L_T \geq 2L$, then ρ_c is

$$\rho_c = R_c \cdot k \cdot L_T \quad [\Omega \cdot cm^2] \tag{2}$$

If $L_T < 2L$, then ρ_c is

$$\rho_c = R_c \cdot k \cdot L \quad [\Omega \cdot cm^2] \tag{3}$$

The sheet resistance (R_p) was measured with a four - point probe at IMMS PAS and calculated according to equation [15, 19]:

$$R_p = \frac{U}{I} \cdot K \quad [\Omega/\Upsilon] \tag{4}$$

where: K – a correction factor, which depends on distance of spacing points and wafer size. The value of this factor is equal to 4.5324 for wafer of size 50 x 50 mm^2 and distances between gauging points about 1 mm

Quantitative chemical composition of contacts is presented in Table 4.

Table 4.
Elements concentrations (wt.% and at.%) of investigated contacts

No	Symbol	Element	Wt. [%]	At. [%]
1	A1	Mg	01.88	07.82
		Ag	98.12	92.18
2	A2	Ag	100.00	100.00

3. Results and discussion

Due to etching in a alkaline solution (30% KOH), approximately 7.5 μm of material on both sides of the wafers was removed.

Sheet resistance was measured using automatic four-point probe, which is a basic method applied to control the diffusion process in the photovoltaic industry. The selected wafers were measured at nine points and the results (mean values) of measurements are presented in Table 5. The emitter with a sheet resistance was equal to 50 $[\Omega/\Upsilon]$ is optimal for screen printing technology.

Table 5.
Mean value of sheet resistance obtained using a four -point probe

No	Symbol	Type	Sheet resistance (R_p) $[\Omega/\Upsilon]$
1	A1	Monocrystalline solar cells with TiO_x	50
2	A2		50

After diffusion from $POCl_3$, the wafers were covered by phosphorous-silicate glass ($xSiO_2 \cdot yP_2O_5$) and have donor-doping layer on both sides and edges.

As a result of passivation process a thin layer of silicon dioxide (SiO_2) of controlled thickness (20 nm) was achieved. The antireflection coating of TiO_x of 80 nm in thickness was accomplished by means of CVD method.

3.1. Contact parameters deduced from TLM

One testing structure was realized on wafer (5 cm x 5 cm). The testing structure consisted of five identical contacts. The contacts were in a shape of thin paths of width equal to 20 mm and length equal 10 mm. Each pair of contacts was separated by a variable distance marked: d_1=20 mm, d_2=10 mm, d_3=5 mm, d_4=2.5 mm. The obtained values of resistance are

presented in Table 6, while the values of electric parameters such as: R_c, L_T and ρ_c are shown in Table 7. The resistance calculations of front contact are presented in turn in Figures 10 and 11. Figs. 12 and 13 present the results of chemical composition analysis performed by EDS method from micro areas.

Table 6.
Values of total resistance between two contacts space by different distances

Sample symbol	I [mA]	R_T [Ω]			
		d_1 [cm]	d_2 [cm]	d_3 [cm]	d_4 [cm]
A1	10	18.32	30.80	55.75	105.65
	30	18.78	31.25	56.20	106.10
	60	19.31	31.79	56.74	106.64
A2	10	30.66	43.13	68.08	117.98
	30	34.89	47.37	72.32	122.22
	60	31.39	43.86	68.81	118.71

Table 7.
Values of electric parameters (R_c, L_T and ρ_c)

Sample	I	R_C	L_T	ρ_c	Performed condition: $L_T \geq 2L$ or $L_T < 2L$
	[mA]	[Ω]	[cm]	[mΩcm^2]	
A1	10	2.92	0.29	0.86	$L_T \geq 2L$
	30	3.15	0.33	1.05	
	60	3.42	0.39	1.32	
A2	10	9.09	1.09	9.94	$L_T \geq 2L$
	30	11.21	1.55	17.37	
	60	9.46	1.37	12.97	
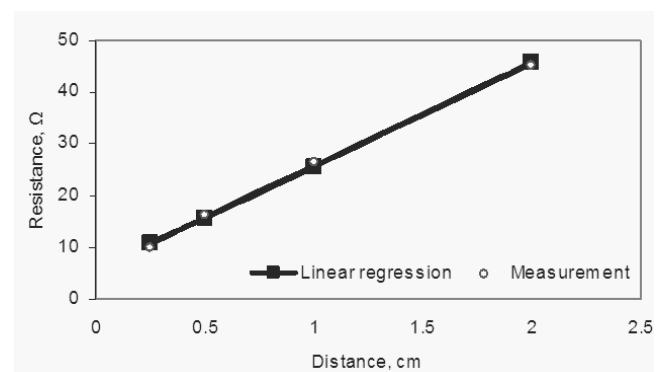
Fig. 10. Resistance versus distance; I=10 mA (example)
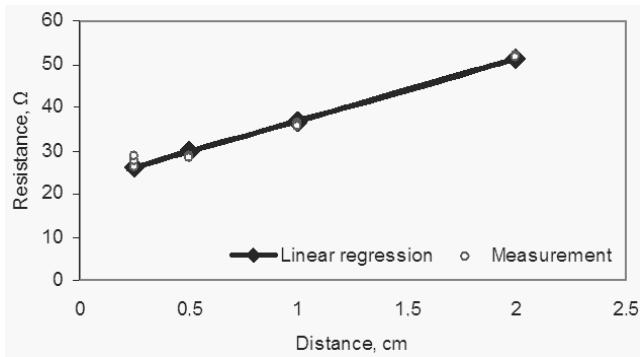
Fig. 11. Resistance versus distance; I=30 mA (example)

SEM images of a path of one contact layer prepared by screen printing using two different pastes are presented in Figures 12 a b and 13 a b c together with corresponding results of EDS analysis.

Howeover, the melted layer of electrode was fractured (Fig. 13), so in order to obtain a better wettability of nano - paste to silicon wafer a ceramic glaze (SiO_2) should be added to it. The sintering electrode obtained from PV 145 paste had a homogenous structure (Fig. 12 a).

a)

b)

c)
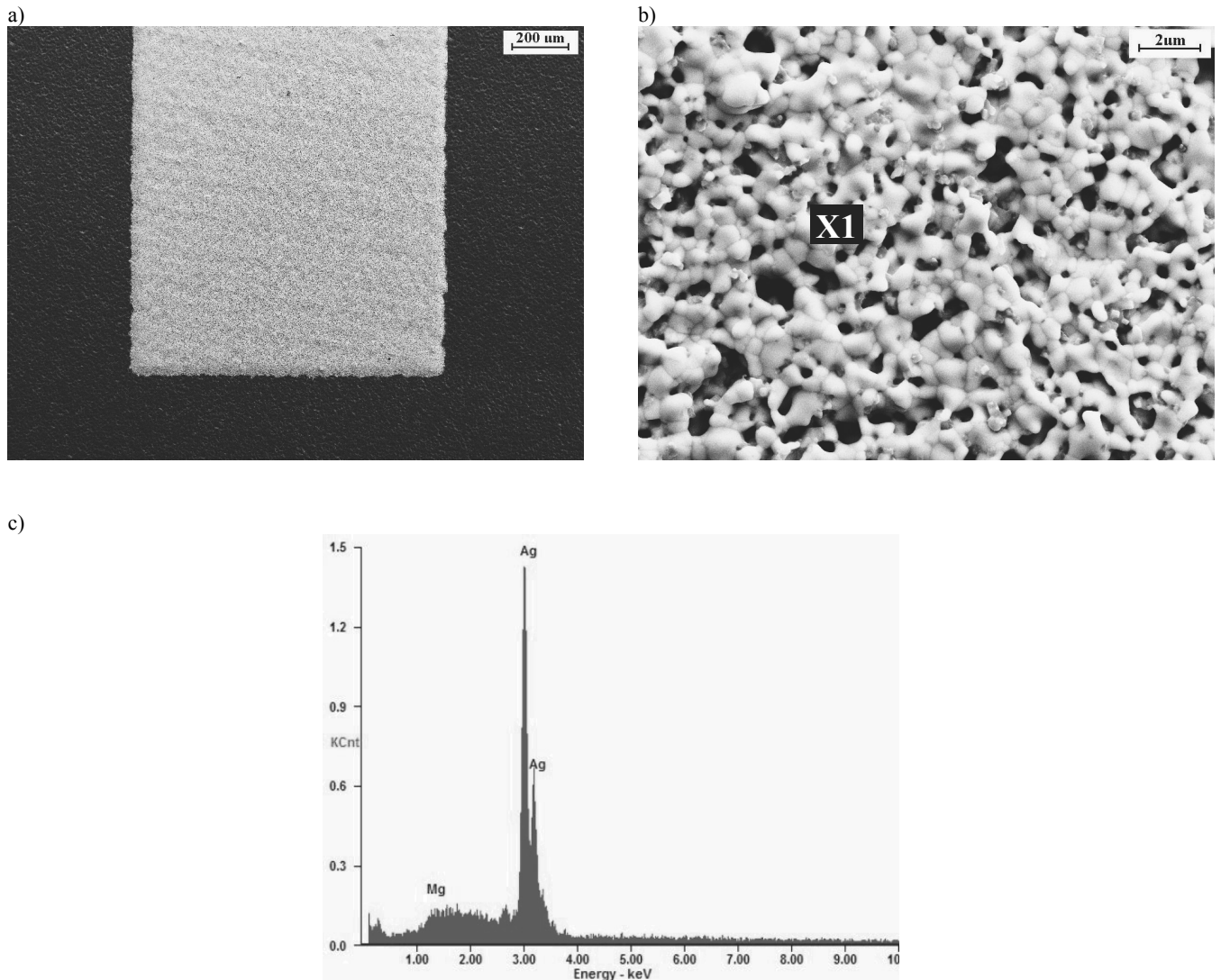
Fig. 12. a), b) SEM images of a path of one contact layer prepared by screen printing (PV 145 paste), c) EDS spectrum from X1 area

a)

b)

c)

d)
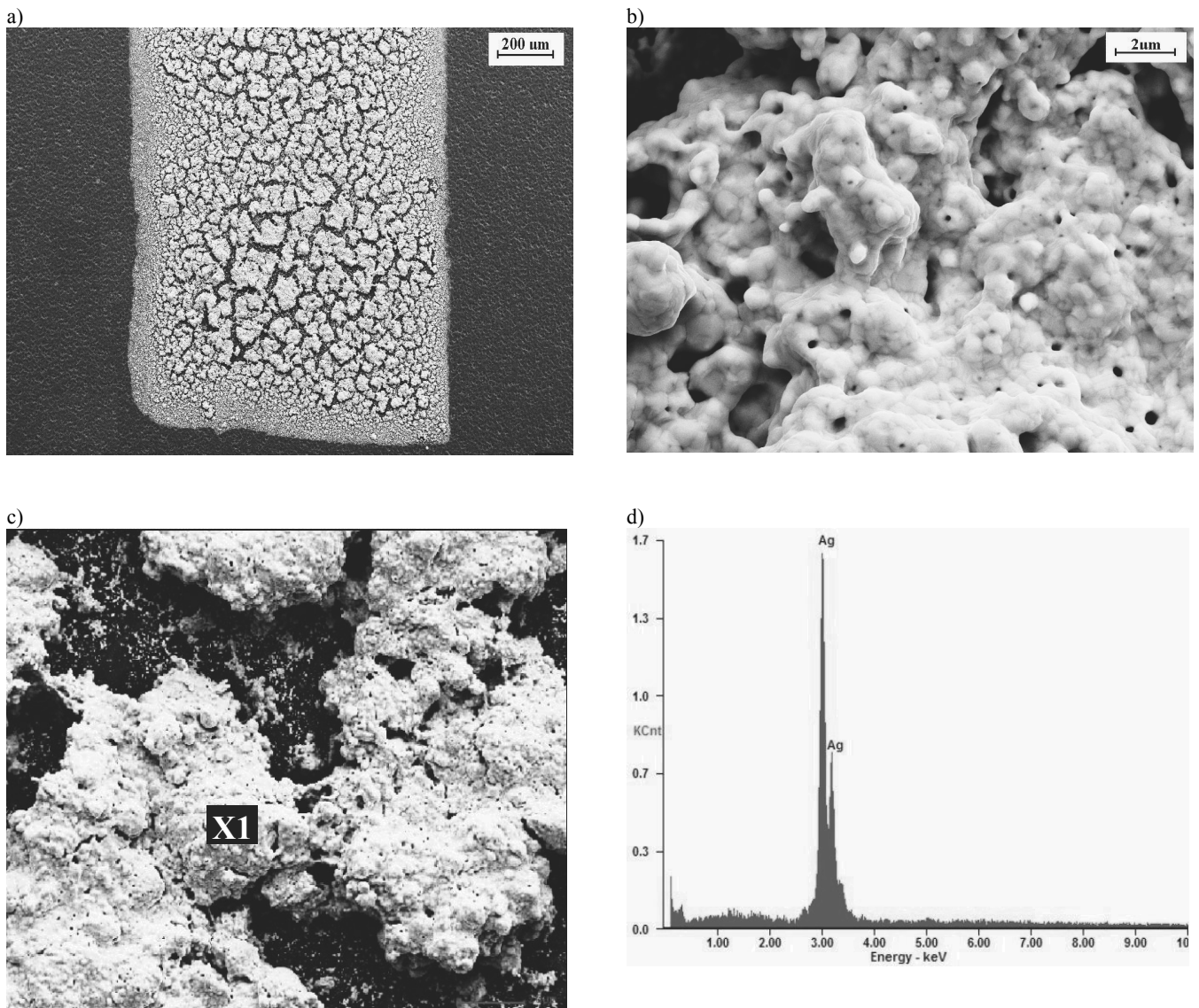
Fig. 13. a, b, c) SEM images of a path of one contact layer prepared by screen printing (nano-paste), d) EDS spectrum from X1 area

4. Summary

The aim of the paper was to optimize co-firing parameters of metal screen printed front contacts on monocrystalline silicon solar cells. The contacts parameters were obtained using Transmission Line Model. It was found during experiments with using screen printing method to form front electrodes that the nano silver paste was the worst distributed on the silicon surface by the squeegees. The standard silver PV 145 paste was well distributed on the silicon surface by the squeegees. A very good screen printed silver contact (PV145 paste) is obtained with a drying at 130ºC for 15 minutes and co – firing at 920˚C. The specific contact resistance is better in a case of PV145 paste rather than a silver nano-paste, but this can be cased by co-firing nano-paste with too low temperature and printed only one layer. Macroscopic observation does not show any difference between both a standard silver PV145 paste and a nano-paste.

A simple industrial procedure for producing silver front contacts on monoctystalline silicon has been developed.

Acknowledgements

References

[1] T. Burakowski, T. Wierzchoń, Surface engineering of metals. WNT, Warsaw, 1995.

[2] M. Alemán, A. Streek, P. Regenfuβ, A. Mette, R. Ebert, H. Exner, S. W. Glunz, G. Willeke, Laser micro-sintering as a new metallization technique for silicon solar cells, Proceedings of the 21st European Photovoltaic Solar Energy Conference, Dresden, Germany, 2006 (CD-ROM).

[3] T. Petch, P. Regenfuβ, R. Ebert, L. Hartwig, S. Klötzer, T. Brabant, H. Exner, Industrial laser micro sintering, Rapid Prototyping Journal 11 (2004) 18-25.

[4] D.M. Huljic, S. Thhormann, R. Preu, R. Lüdemann, G. Willeke, Pad printing front contacts for c-Si solar cells-a technological and economical evaluation, Proceedings of the 29th IEEE PVSC, New Orleans, Louisiana, 2002, 126-129.

[5] F.C. Krebs, Fabrication and processing of polymer solar cells: A review of printing and coating techniques, Solar Energy Materials and Solar Cells 93 (2009) 394-412.

[6] S.W. Glunz, J. Dicker, M. Esterie, M. Hermie, J. Iserberg, F. Kamerewerd, J. Knobloch, D. Kray, A. Leimenstoll, F. Lutz, D. Oβwald, R. Preu, S. Rein, E. Schäffer, C. Schetter, H. Schmidhuber, H. Schmidt, M. Steuder, C. Vorgrimler, G. Willeke, High-efficiency silicon solar cells for low-illumination applications, Proceedings of the Photovoltaic Specialists Conference, New Orleans, 2002, 450-453.

[7] W. Neu, A. Kress, W. Jooss, P. Fath, E. Bucher, Low-cross multicrystalline back-contact silicon solar cells with screen printed metallization, Solar Energy Materials and Solar Cells 74/1-4 (2002) 139-146.

[8] V. Gazus, K. Feldrapp, R. Auer, R. Brendel, M. Schultz, Dry processing of silicon solar cells in a large area microwave plasma reactor, Solar Energy Materials and Solar Cells 77 (2002) 277-284.

[9] N.B. Mason, O. Schultz, R. Russel, S.W. Glunz, W. Warta, 20.1% efficient large area cell on 140 micron thin silicon wafer, Proceedings of the 21st European Photovoltaic Solar Energy Conference EU PVSEC'06, Dresden, Germany, 2006, 521.

[10] M.A. Green, A.W. Blakers, S.R. Wenham, et al., Improvements in silicon solar cell efficiency, Proceedings of the 19th IEEE Photovoltaic Specialists Conference PVSC'85, Las Vegas, 1985, 39-42.

[11] L.A. Dobrzański, A. Drygała, P. Panek, M. Lipiński, P. Zięba, Development of the laser method of multicrystalline silicon surface texturization, Archives of Materials Science and Engineering 38/1 (2009) 5-11.

[12] L.A. Dobrzański, A. Drygała, Laser texturization in technology of multicrystalline silicon solar cells, Journal of Achievements in Materials and Manufacturing Engineering 29/1 (2008) 7-14.

[13] L.A. Dobrzański, A. Drygała, Processing of silicon surface by Nd:YAG laser, Journal of Achievements in Materials and Manufacturing Engineering 17 (2006) 321-324.

[14] L.A. Dobrzański, A. Drygała, P. Panek, M. Lipiński, P. Zięba, Application of laser in silicon surface processing, Journal of Achievements in Materials and Manufacturing Engineering 24/2 (2007) 179-182.

[15] L.A. Dobrzański, M. Musztyfaga, A. Drygała, P. Panek, K. Drabczyk, P. Zięba, Manufacturing solar cells using screen painting, Proceedings of the 1st KKF Conference, Krynica-Zdrój, 2009 (CD-ROM).

[16] A. Klimpel, A. Rzeźnikiewicz, Ł. Janik, Study of laser welding of copper sheets, Journal of Achievements in Materials and Manufacturing Engineering 20 (2007) 467-470.

[17] A. Goetzberg, J. Knobloch, B. Voß, Crystalline silicon solar cells. John Wiley and Sons, 1994.

[18] E.G. Woelk, H. Kräutle, H. Beneking, Measurement of low resistance ohmic contacts on semiconductors, IEEE Transactions on Electron Device 33/1 (1986) 19-22.

[19] A. Drygała A. The influence of laser texturing on photovoltaic properties of polycrystalline silicon, Doctoral dissertation, The main library of Silesian University, Gliwice, 2007.